Neuroscience 158 (2009) 1364–1377

EXCITATORY TONUS IS REQUIRED FOR THE SURVIVAL OF GRANULE CELL PRECURSORS DURING POSTNATAL DEVELOPMENT WITHIN THE CEREBELLUM

A. K. KANUNGO,[a] N. LIADIS,[b] J. ROBERTSON,[c] M. WOO[b] AND J. T. HENDERSON[a]*

[a]*Department of Pharmaceutical Sciences, University of Toronto, 144 College Street, Room 938, Toronto, Ontario, Canada M5S 3M2*

[b]*Department of Medical Biophysics, Ontario Cancer Institute, University of Toronto, Ontario, Canada M5G 2M9*

[c]*Department of Pathology and Molecular Medicine, McMaster University, Hamilton, Ontario, Canada L8N 3Z5*

Abstract—In addition to protective effects within the adult central nervous system (CNS), *in vivo* application of *N*-methyl-D-aspartate inhibitors such as (+) MK-801 have been shown to induce neurodegeneration in neonatal rats over a specific developmental period. We have systematically mapped the nature and extent of MK-801-induced neurodegeneration throughout the neonatal murine brain in order to genetically dissect the mechanism of these effects. Highest levels of MK-801-induced neurodegeneration are seen in the cerebellar external germinal layer; while mature neurons of the internal granule layer are unaffected by MK-801 treatment. Examination of external germinal layer neurons by electron microscopy, terminal deoxynucleotidyl transferase biotin-dUTP nick end labeling (TUNEL) and bromodeoxyuridine (BrdU) labeling, and caspase-3 activation demonstrate that these neurons die through the process of programmed cell death soon after they exit from the cell cycle. Significantly, ablation of caspase-3 activity completely inhibited the MK-801-induced (and developmental) programmed cell death of external germinal layer neurons. Similar to caspase-3, inactivation of muscarinic acetylcholine receptors *in vivo* using scopolamine inhibited MK-801-induced programmed cell death. By contrast, the GABAergic agonist diazepam, either alone or in combination with MK-801, enhanced programmed cell death within external germinal layer neurons. These data demonstrate that, *in vivo*, cerebellar granule neurons undergo a dramatic change in intracellular signaling in response to molecules present in the local cellular milieu during their first 24 h following exit from the cell cycle.

Key words: MK-801, diazepam, scopolamine, apoptosis, granule neurons, caspase-3.

*Correspondence to: J. T. Henderson, University of Toronto, Faculty of Pharmacy, 144 College Street, Room 903, Toronto, Ontario, Canada M5S 3M2. Tel: +1-416-946-5571; fax: +1-416-978-8511.
E-mail address: jeff.henderson@utoronto.ca (J. T. Henderson).

Abbreviations: ANOVA, analysis of variance; BrdU, bromodeoxyuridine; CNS, central nervous system; DAB, 3,3-diaminobenzidine; E, embryonic day; EGL, external germinal layer; EM, electron microscopy; GIRK, G-protein sensitive inwardly rectifying potassium channel; GPBS, 5% goat serum in PBS; IGL, internal granule layer; NMDA, *N*-methyl-D-aspartate; P, postnatal day; PCD, programmed cell death; RT, room temperature; TUNEL, terminal deoxynucleotidyl transferase biotin-dUTP nick end labeling.

0306-4522/09 © 2009 IBRO. Published by Elsevier Ltd. All rights reserved.
doi:10.1016/j.neuroscience.2008.10.062

Programmed cell death (PCD) is an evolutionarily conserved process of cellular suicide (Yuan, 2006) which plays a key role in normal development (Baehrecke, 2002), and in acute and chronic neuronal loss following injury to the mammalian central nervous system (CNS) (Mattson, 2000; Hara and Snyder, 2007). One well-recognized form of neurodegenerative PCD within the adult CNS arises following excessive activation of glutamate receptors, resulting in elevated calcium influx and downstream caspase activation (Nicholls and Ward, 2000; Mattson, 2003). Blockade of *N*-methyl-D-aspartate (NMDA) receptors *in vivo* using antagonists such as the non-competitive, open-channel blocker MK-801, has been shown to confer neuroprotection from several forms of glutamate-related injury (McIntosh et al., 1989; Greensmith et al., 1994; Nicholls, 2004). In contrast, blockade of NMDA receptors during the early postnatal period is associated with a developmental vulnerability to neurodegeneration (Ikonomidou et al., 1999). This developmental window (postnatal days (P)3–P7 in rodents) coincides with an enhanced period of synaptogenesis and brain growth (Gottlieb et al., 1977; Dobbing and Sands, 1979; Hahn et al., 1983). This effect is of interest clinically, as drugs which inhibit NMDA receptors such as ethanol, phencyclidine, and anesthetics like ketamine and nitrous oxide, could potentially induce neuronal damage if fetal exposure to a sufficient dosage occurs during the critical developmental window (Bayer et al., 1993; Ikonomidou et al., 2000). Previous studies have demonstrated that these agents affect several levels of the developing CNS (Ikonomidou et al., 2000). Within the cerebellum, short term *in vitro* inhibition of NMDA signaling disrupts the migration of immature granule cells (Komuro and Rakic, 1993); however, the mechanistic consequence of sustained periods of NMDA receptor inactivation on the developing cerebellum has not been well characterized *in vivo*.

The cerebellum is principally composed of five neuronal subtypes: Purkinje and granule neurons, together with basket, stellate and Golgi interneurons. Granule cells arising from progenitors initially develop within the external germinal layer (EGL) prior to birth (Goldowitz and Hamre, 1998; Middleton and Strick, 1998; Carletti and Rossi, 2008). Following their last mitotic division, immature granule neurons migrate along Bergmann glia, through the Purkinje cell layer, to their final location within the internal granule layer (IGL). Analysis of the EGL reveals that, along with cell proliferation, a substantial amount of PCD occurs during normal development in rodents and humans (Tanaka and Marunouchi, 1998; Abraham et al., 2001). However, little is known regarding the mechanism of these effects.

Here we demonstrate that MK-801-induced death within the neonatal EGL occurs via PCD; and caspase-3 is both necessary and sufficient to regulate this process. During normal development, a significant fraction of PCD within the EGL (but not the IGL) requires caspase-3 activity; despite detectable activation of caspase-3 at both sites. Analysis of coincident bromodeoxyuridine (BrdU)/terminal deoxynucleotidyl transferase biotin-dUTP nick end labeling (TUNEL) labeling following MK-801 treatment indicates that a sizable fraction of granule cells undergoing PCD within the EGL, do so proximal to their last mitotic division. Finally, *in vivo* studies using scopolamine and diazepam suggest that sub-threshold levels of neuronal responsiveness may initiate the process of PCD in immature granule neurons of the EGL.

EXPERIMENTAL PROCEDURES

Animals and drug treatment

Seven-day-old *Casp3*$^{-}$/$^{-}$ mice were obtained from timed mating of our caspase-3 stock (heterozygous/heterozygous and heterozygous/homozygous intercrosses), and genotyped by PCR analysis as previously described (Woo et al., 1998). Mice were housed in a gnotobiotic facility at the Ontario Cancer Institute (Toronto, Canada). All procedures were in accordance with the Canadian Council on Animal Care (Guide to the Care and Use of Experimental Animals, Vol. 1, 2nd Ed., 1993) and the Animals for Research Act (Ontario, Canada, revised 1990), and approved by the University of Toronto Faculty Advisory Committee on Animal Services. All efforts were made to minimize the number of animals used and their suffering. For the studies described, *Casp3*$^{-}$/$^{-}$ mutants and littermate controls were examined on both inbred (C57BL/6J) and outbred (CD1) backgrounds. For the analyses shown, no significant differences in response to MK-801 was observed between *Casp3*$^{+/+}$ and *Casp3*$^{+}$/$^{-}$ littermates on either inbred or outbred backgrounds. For initial MK-801 studies in wild-type animals, 129Sv/IMJ strain mice were also examined. P7 mice were injected s.c. with either saline or MK-801 [(+) MK-801, 5 mg/kg body weight, Research Biochemicals International (RBI), Natick, MA, USA] alone, scopolamine (0.3 mg/kg, RBI), diazepam (10 mg/kg, RBI), or a combination of these drugs. S.c. injections were given at t=0, 8, and 16 h with animals killed at t=24 h. Brains were removed and fixed in 4% paraformaldehyde in 0.1 M PBS at 4 °C overnight, while tail samples were collected for genotyping. The cerebella were subsequently dissected, and either embedded in paraffin, or processed for frozen sections (caspase-3 immunohistochemistry) at 15–30 μm. Paraffin samples were cut at a thickness of 7 μm in serial sets at intervals of 150 μm.

Electron microscopy (EM)

Cerebellar samples for EM were fixed in 2% glutaraldehyde, 2% paraformaldehyde in 0.1 M sodium cacodylate buffer (pH 7.4), at 4 °C for 12 h. Samples were subsequently impregnated with 1% osmium tetroxide, and 2% uranyl acetate in 0.1 M PBS for 1 h, then dehydrated in a series of water/ethanol and ethanol/propylene oxide baths prior to embedding in Spurr resin. Seventy nanometer ultrathin sections were then obtained and placed onto formvar-coated grids for examination on a Phillips CM 100 electron microscope equipped with a Kodak QRS 1050 digital camera.

For EM blocks, thin (1 μm) sections were also obtained and stained with Toluene Blue for analysis by light microscopy in order to aid in the positional orientation of EM photos.

Immunohistochemical analyses

Paraffin sections were de-waxed and TUNEL positive cells were identified using the TUNEL assay (FITC-TUNEL cell death assay kit, Roche Biochemicals, Indianapolis, IN, USA), in accordance with the manufacturer's instructions. For each set of tissue sections, one positive and two negative control slides were processed with each batch to verify the fidelity of TUNEL staining. Positive TUNEL controls consisted of sections taken from gamma-irradiated (2 Gy) E13.0 embryos (TUNEL-positive cells: cortical neuro-epithelium). Negative controls consisted of sections from non-irradiated E13.0 embryos and an irradiated embryo slide in which terminal deoxynucleotidyl transferase (TdT) had been eliminated from the TUNEL reaction mixture. For analysis of activated caspase-3 (New England Biolabs (NEB), Ipswitch, MA, USA, 1:200), tissues were cryoprotected in sucrose overnight at 4 °C then embedded in OCT the next day. Samples were sectioned at 15 or 30 μm on a Leitz model CM3050 cryostat. For peroxide-based immunohistochemistry of tissue sections, endogenous peroxide activity was first quenched through exposure to a freshly prepared solution of 3% H_2O_2 in 100% methanol for 30 min at room temperature (RT). Samples were then blocked in 5% goat serum, 0.2% Tween-20 in 0.1 M PBS (pH 7.4) for 1 h prior to overnight incubation in primary antibody at 4 °C. Sections were then washed three times 5 minutes and incubated in biotinylated secondary antibody (Vector Laboratories, Burlingame, CA, USA, 1:200) for 2 h at RT, followed by washing and incubation with streptavidin HRP (Vector Laboratories) at 1:100 for 1 h at RT. Sections were then visualized with 3,3-diaminobenzidine with nickel enhancement (DAB, Vector Laboratories). For dual visualization of TUNEL and activated caspase-3, microwave/citrate buffer antigen retrieval was first performed on dewaxed serial paraffin sections. The sections were allowed to cool for 30 min in PBS, then blocked (as described above) for 1 h, and incubated overnight at 4 °C in anti-activated caspase-3 (NEB, 1:100) antibody. Sections were then washed three times 5 min and incubated in goat anti-rabbit Alexa 546 (Molecular Probes, Carlsbad, CA, USA, 1:200) for 2 h at RT. After washing, sections were then visualized for immunofluorescence. No significant difference was observed in the number of neurons demonstrating immunoreactivity for activated caspase-3 on paraffin sections in comparison to frozen sections. The sections were then digested with 10 mg/mL proteinase K for 15 min, followed by TUNEL as per the manufacturer's protocol. Note that proteinase K digestion (required for TUNEL) prior to this point resulted in damage to the epitope recognized by the antisera directed against activated caspase-3. No significant difference in the number of TUNEL positive cells was observed between sections which received antigen retrieval, and those that did not.

BrdU labeling

A single injection of BrdU (100 mg/kg, Sigma Aldrich, Oakville, ON, Canada) was given s.c. to P7 mice at t=12 or t=22 or t=23 h following MK-801 injection (t=0, 8, 16 h, mice killed at t=24 h). Sets of 7 μm paraffin sections were then obtained through the cerebellum in the sagittal plane at intervals of 150 μm through the central third of the cerebellum (distance covered: 1050 μm to either side of the cerebellar midline for each animal). For immunohistochemistry, sections were de-waxed, and endogenous peroxidase activity quenched as described above. Samples were incubated with 0.01% pepsin (Sigma Aldrich) in 0.01 N HCl for 15 min at 37 °C and denatured in 2 N HCl for 45 min. Sections were then neutralized in a solution of 0.1 M sodium borate (pH 8.5). After washing, slides were incubated in a solution of 5% goat serum in PBS (GPBS) for 30 min at RT. This was followed by incubation in a 1:30 dilution of mouse monoclonal anti-BrdU (Becton-Dickinson, Mississauga, ON, Canada, 347580) in GPBS overnight at 4 °C in a humidified chamber. The following day, slides were processed for DAB visualization as described above.

Imaging analysis

Microscope images were captured by SimplePCI (version 5.3, Compix Inc.) on a Nikon Eclipse E1000 fluorescent microscope equipped with a Hamamatsu C4742-95 camera for fluorescence microscopy and a Nikon DS-Fi1 color camera for brightfield analysis. Images were assembled and adjusted for brightness and contrast using Photoshop 7.0 (Adobe Systems). For regional TUNEL counts, numbers of TUNEL positive cells within an area equivalent to 1 mm^2 were determined for each stereotactic section obtained within the identified neural locus. For TUNEL counts of the cerebellum, two separate regions (within cerebellar lobes VI and VII) of 1 mm contiguous length were assessed for numbers of TUNEL-positive cells throughout the full height of the EGL (P8 $\sim$150 μm) for each stereotactic section. For IGL analyses, counts were determined in two regions (independent cerebellar lobes) representing a total area of 1 mm^2 for each stereotactic section. Total TUNEL-positive counts were reported for each neural locus as numbers of positive cells/mm^2. Procedures to determine counts of BrdU-positive cells within the cerebellar EGL and IGL were as indicated above for TUNEL.

Statistical analysis

Data are expressed as mean$\pm$S.E.M. The Student's *t*-test was used for data in which only two groups were compared. Statistical significance was determined at * $P<0.05$ and ** $P<0.01$. Tests of normality, distribution and variance homogeneity were performed to ensure that the assumptions required for a standard parametric analysis of variance (ANOVA) were satisfied. An ANOVA followed by Fisher's PLSD post hoc test was performed to compare the data from multiple groups; statistical significance was assessed at * $P<0.05$. Statistical analysis was performed on the data obtained using GraphPad Prism (version 3.0).

RESULTS

NMDA receptor blockade selectively enhances cell death within the EGL of the murine cerebellum

MK-801 has previously been shown to induce CNS degeneration over a specific developmental window in rats (Ikonomidou et al., 1999). Mice rather than rats were employed for our analysis of MK-801-mediated effects in the CNS, due their greater potential for genetic uniformity, extensive genetic mapping, and malleability with respect to genetic recombination (Jackson and Abbott, 1999). To verify the level and extent of MK-801-induced degeneration, inbred (C57BL/6J) or outbred (CD1) mice were treated with 0.5 mg/kg MK-801 at $t=0$, 8 and 16 h, and killed at $t=24$ h. Wild-type mice were initially treated with MK-801 or saline vehicle at embryonic day (E) 18.5, or P3, 7, 10 or 14. The greatest extent of MK-801-induced cell death within the murine CNS was observed between P7-8 (Supplementary Fig. 1) in agreement with previous reports in rat (Ikonomidou et al., 1999), and this period was employed for all further studies. MK-801 treatment prior to E18.5, or following P14, did not result in a significant elevation in cell death within the CNS compared with controls for any of the murine lines tested (C57BL/6J, 129Sv/IMJ, CD1, data not shown). We then proceeded to extend the previous analysis of MK-801-induced degeneration in rodents (Ikonomidou et al., 1999), by performing an extensive examination of cell death within the cerebellum.

Counts of TUNEL-positive nuclei were determined from serial sagittal sections of the medial vermal lobes (lobes VI and VII) extending through the central third of the cerebellum (spinocerebellum) for saline- (Fig. 1A) and MK-801- (Fig. 1B) treated mice at P8 (section interval 150 μm, $N=9$ and 12 animals per respective group). As shown in Fig. 1A, and summarized in Fig. 1C, both the EGL, and the IGL exhibit significant developmental PCD during this period. While treatment with MK-801 dramatically exacerbated the level of cell death within the cerebellum, this effect was cell type-specific, principally affecting the EGL (Fig. 1B and 1C). Indeed the highest densities of TUNEL-positive cells observed within any region of the murine CNS following MK-801 treatment were observed within the EGL of the cerebellum.

During the early postnatal period, the EGL consists entirely of granule cell progenitors and pre-migratory granule neurons proximal to the pial surface, and ventrally migrating granule neurons (Carletti and Rossi, 2008). To understand the nature by which cells of the EGL underwent cell death, cerebella of MK-801 and saline-treated mice were examined using EM and optical microscopy. As shown in Fig. 2, analysis of EM and thin sections from the EGL demonstrated that treatment with MK-801 resulted in a substantial increase in the presence of degenerating neurons which exhibited features of chromatin compaction (Fig. 2D), nuclear condensation, and cellular blebbing (Fig. 2G, H); morphological features consistent with the process of PCD. In combination with the TUNEL results obtained, these findings suggest that the neuronal degeneration observed within the EGL following MK-801 treatment is the result of PCD.

To further define the nature of the cell death observed within the EGL following MK-801 treatment, cerebellar frozen sections were stained for activated caspase-3 (see cerebellar overview, Fig. 3A). As shown in Fig. 3, mice treated with saline typically exhibit low numbers of activated caspase-3 positive cells within the EGL (Fig. 3B, and enlargement 3C). By contrast, treatment with MK-801 resulted in a substantial increase in the numbers of cells expressing activated caspase-3 within the EGL (Fig. 3D and enlargement 3E; summarized in Fig. 3F). Interestingly, double labeling with TUNEL and activated caspase-3 demonstrated that a small number of TUNEL-positive cells within the EGL were observed to be negative for activated caspase-3 irrespective of saline or MK-801 treatment (Fig. 3G and 3H, respectively). However, the majority of TUNEL-positive cells within the EGL demonstrated caspase-3 activation following MK-801 treatment. Thus dying cells following MK-801 administration were observed to be TUNEL-positive, expressed activated caspase-3, and showed morphologic changes indicative of PCD. Taken together, these date indicate that inhibition of NMDA receptor function within the EGL at P7-8 triggers the induction of PCD.

NMDA blockade induces PCD in granule cell progenitors

To further characterize that population of EGL neurons which undergo PCD following MK-801 treatment, P7-8 mice were treated with BrdU at various time points following the initiation of MK-801 treatment. BrdU was utilized as a marker of cell division due to its ability to incorporate during the S (synthesis) phase of DNA replication over a

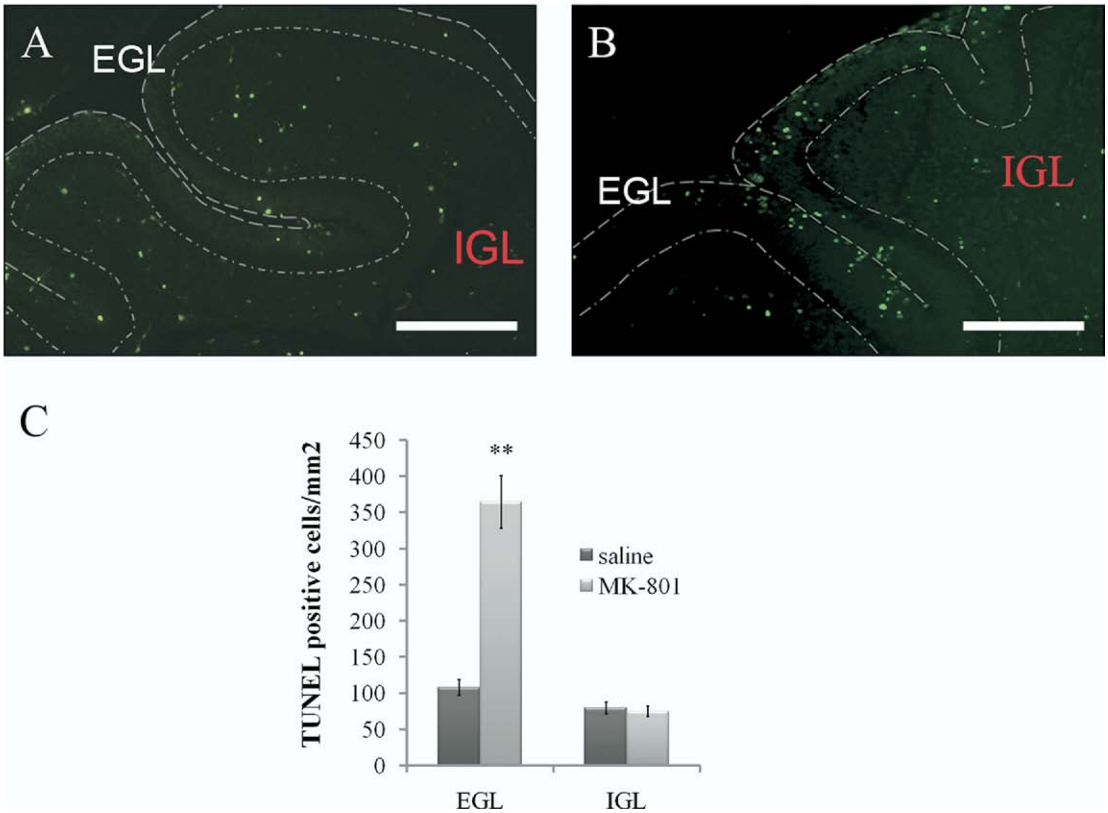

Fig. 1. Examination of MK-801-induced PCD in the murine cerebellum at P8. Sagittal cerebellar cross-sections were examined by TUNEL to determine the distribution of degenerating neurons within the cerebellum at P8. White dashed line (short) delineates the Purkinje cell layer of the cerebellum. White dashed line (long) delineates the outermost border of the cerebellum. (A) Photomicrograph showing the intrinsic level of TUNEL-positive cells within the murine cerebellum at P8 following saline treatment; (B) distribution of TUNEL-positive cells within the murine cerebellum following MK-801 treatment; (C) cumulative plot of the average number of TUNEL-positive nuclei per mm^2 per animal within the murine cerebellum as a function of their distribution within the EGL or IGL of the cerebellum following MK-801 ($N=12$) or saline treatment ($N=9$). Unpaired t-test (** $P<0.01$) demonstrated a significant difference between MK-801- and saline-treated animals within the EGL. Error bars are shown ±S.E.M. For photomicrographs (A) and (B), scale bar=200 μm.

defined temporal window. Animals were injected with a single dose of BrdU at $t=12$ h ($N=5$ animals/group) or $t=23$ h ($N=4$ animals/group) following the initiation of MK-801 treatment. As shown in Fig. 4, MK-801-treated mice injected with BrdU as little as 1 h prior to sacrifice exhibited a substantial reduction in BrdU-labeled cells compared with saline-treated controls in the EGL (Fig. 4A and 4B respectively). The pattern of BrdU labeling seen through the medial third of the cerebellum (lobes VI and VII) following MK-801 treatment is shown in Fig. 4C and 4D. The extent of BrdU labeling for saline and MK-801-treated mice is summarized in Fig. 4E. These data demonstrate that treatment with MK-801 results in a substantial reduction of cells labeled with BrdU 60 min prior to sacrifice within the EGL; indicating the loss of mitotically active granule cell progenitors, pre-migratory granule neurons and a smaller number of migrating granule neurons. A similar trend was observed in mice labeled with BrdU 12 h ($t=12$ h) prior to sacrifice (data not shown). Consistent with the temporal BrdU labeling data, doubly positive BrdU/TUNEL-labeled cells were most frequently observed along the outer limit (active germinal zone) of the EGL for both vehicle (Fig. 5A, and high magnification view in 5C), and MK-801-treated mice (Fig. 5B, and high magnification view in 5D). However, despite differences in the relative magnitude of cell death within the EGL between MK-801-treated mice and vehicle controls, a plot of the percent distribution of TUNEL positive/BrdU negative, versus double positive TUNEL/BrdU cells (Fig. 5E) demonstrates similar distributions between the two groups.

Based upon both the increase in PCD between MK-801 and saline treated mice (3.4-fold, Fig. 1C), and the reduction in BrdU positive cells in MK-801 treated mice compared with controls (2.5-fold, Fig. 4E), one would expect that if MK-801 treatment did not actually alter the normal pathway of death, but simply increased its probability, that the percent distribution of TUNEL/BrdU positive cells of MK-801 versus control values would be 1.4 (3.4/2.4). While the experimentally observed ratio of 1.2 (Fig. 5E) is close to the expected value, this difference may reflect a slightly increased propensity of pre-migratory and migratory granule cells versus granule cell progenitors, to undergo PCD in MK-801-treated mice compared with vehicle-treated controls. Focal treatment with MK-801 in P7-P8 mice did not result in significant long-term morphologic or functional impairments as determined at P28 (functional assays: beam balance, T-bar crossing, rotorod performance at 45 rpm;

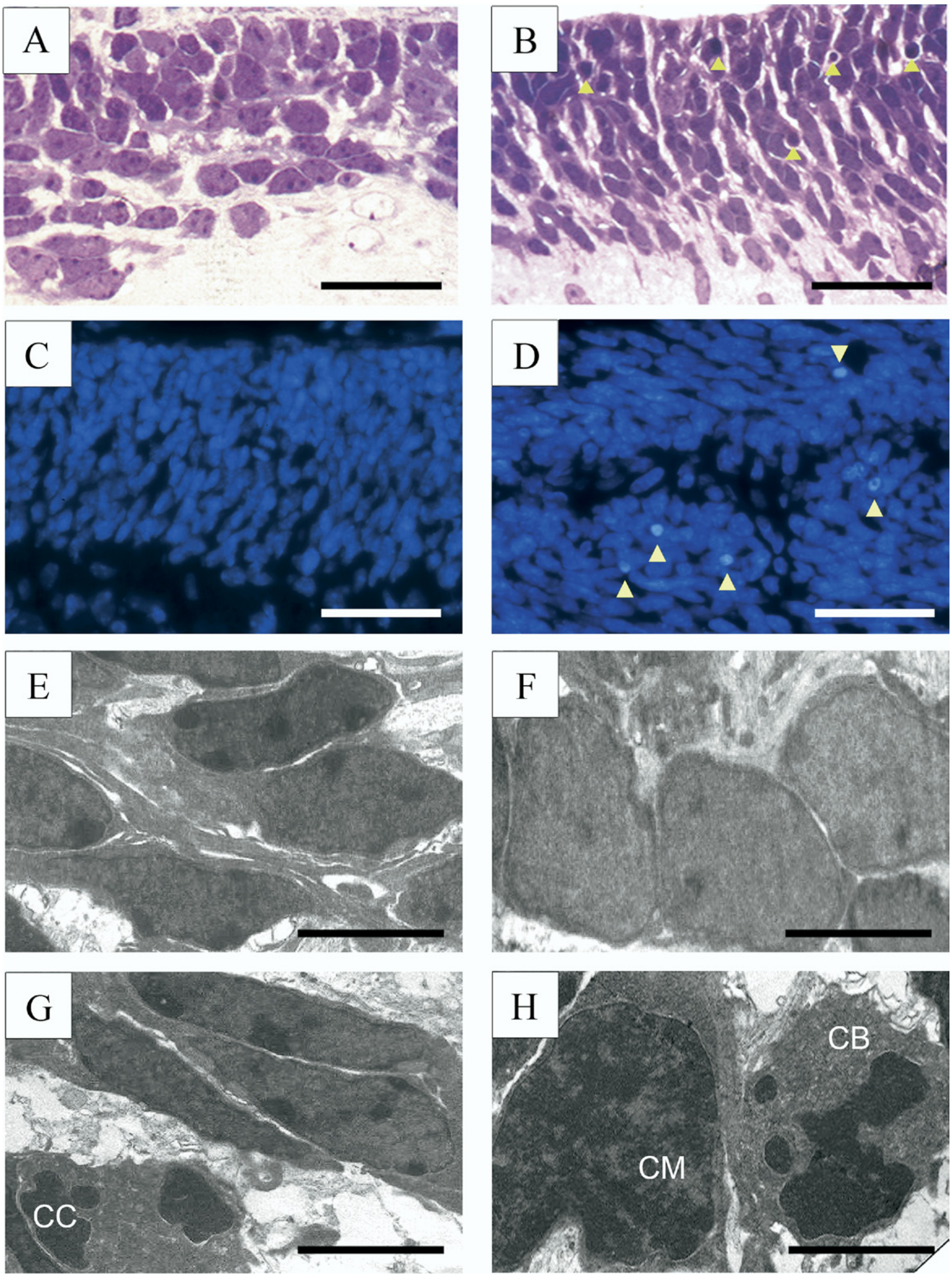

Fig. 2. Morphology of degenerating neurons within the murine EGL following MK-801 treatment at P8. One micron thin sections from the murine EGL were examined at P8 following (A) saline, or (B) MK-801 treatment. (C, D) Hoechst 33258-labeled nuclei from the murine EGL at P8 following (C) saline, or (D) MK-801 treatment. Arrowheads (B, D) denote neurons with compacted nuclei. Examination of the EGL by EM following saline treatment (E, F) demonstrates a predominance of morphologically normal cells; whereas treatment with MK-801 (G, H) resulted in the presence of interspersed cells with nuclei in various stages of chromatin compaction and fragmentation (t=24 h). Early stage chromatin margination/nuclear condensation (CM) into a crescent-shaped electron-dense structure, chromatin compaction (CC), and cytoplasmic membrane blebbing (CB) is indicated in (G, H). Scale bar=40 μm (A, B); 100 μm (C, D); 5 μm (E–H).

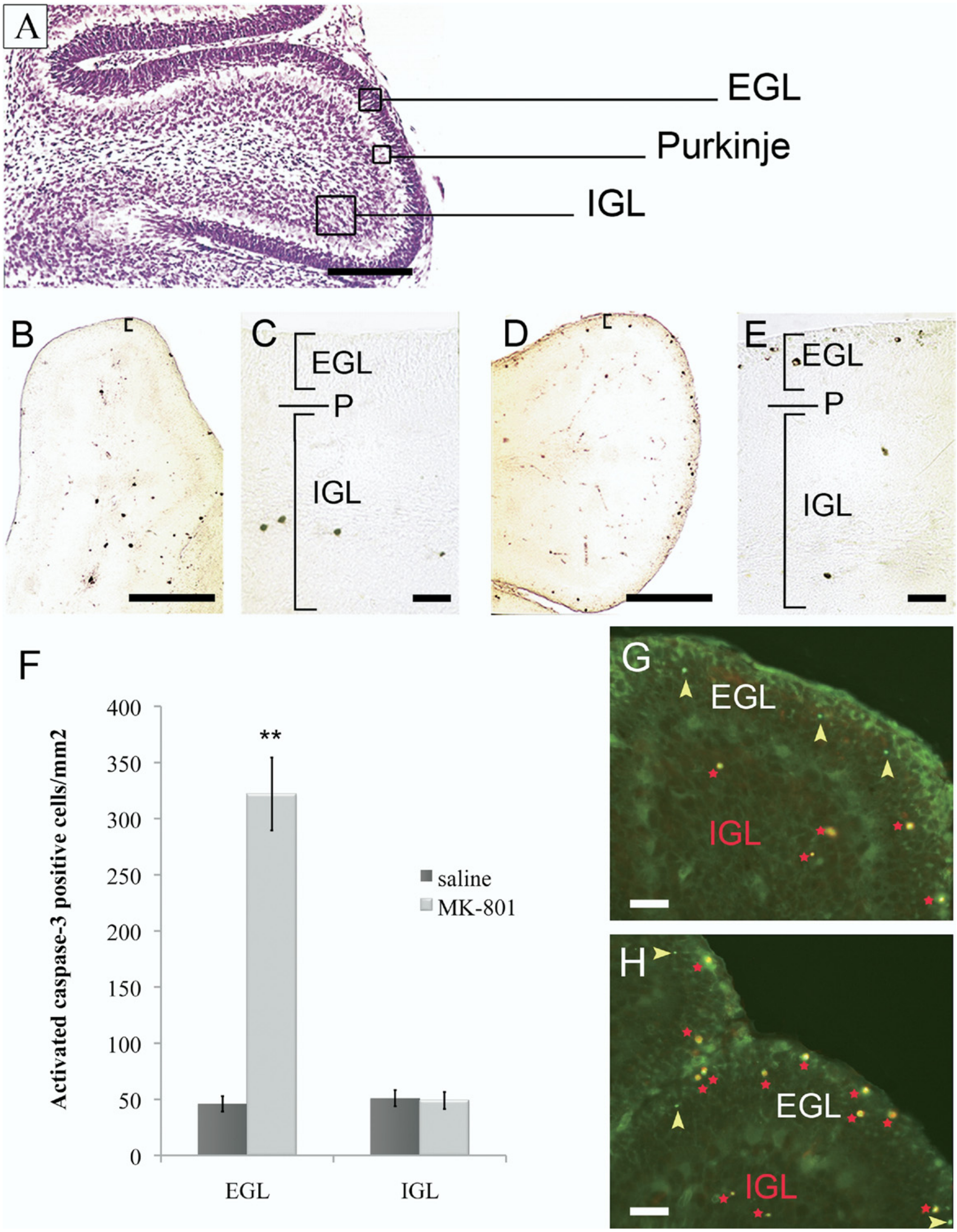

Fig. 3. Caspase-3 activation within the murine cerebellum following MK-801 treatment at P8. The pattern of activated caspase-3 was examined at 24 h following MK-801 or saline treatment. (A) Overview of murine cerebellar morphology at P8. Cross-section was stained with thionin to delineate layers. (B, C) Pattern of activated caspase-3 immunoreactivity within cerebellar lobes following saline treatment: (B) lower magnification overview, (C) higher magnification view. (D, E) Pattern of activated caspase-3 following MK-801 treatment. (D) Lower magnification overview, (E) higher magnification view. Scale bar=400 μm (B, D); 50 μm (C, E). Region of the EGL in (B, D) is indicated by bracket. Position of the EGL, Purkinje cell layer (P), and IGL is indicated in (C, E). (F) Cumulative plot of the average number of cells demonstrating activated caspase-3 immunoreactivity per mm^2 per animal within the murine cerebellum as a function of their distribution the EGL or IGL following MK-801 (N=5) or saline treatment (N=5). Unpaired t-test (** P<0.01) demonstrated a significant difference between MK-801 and saline-treated animals within the EGL. (G, H) Co-visualization of TUNEL (green) and activated caspase-3 (red) immunoreactivity within the cerebellum following saline (G), and MK-801 (H) treatment. Double-positive TUNEL/activated caspase-3 cells within the EGL are indicated by stars. TUNEL-positive/activated caspase-3 negative cells are denoted by arrowheads. Scale bar=50 μm.

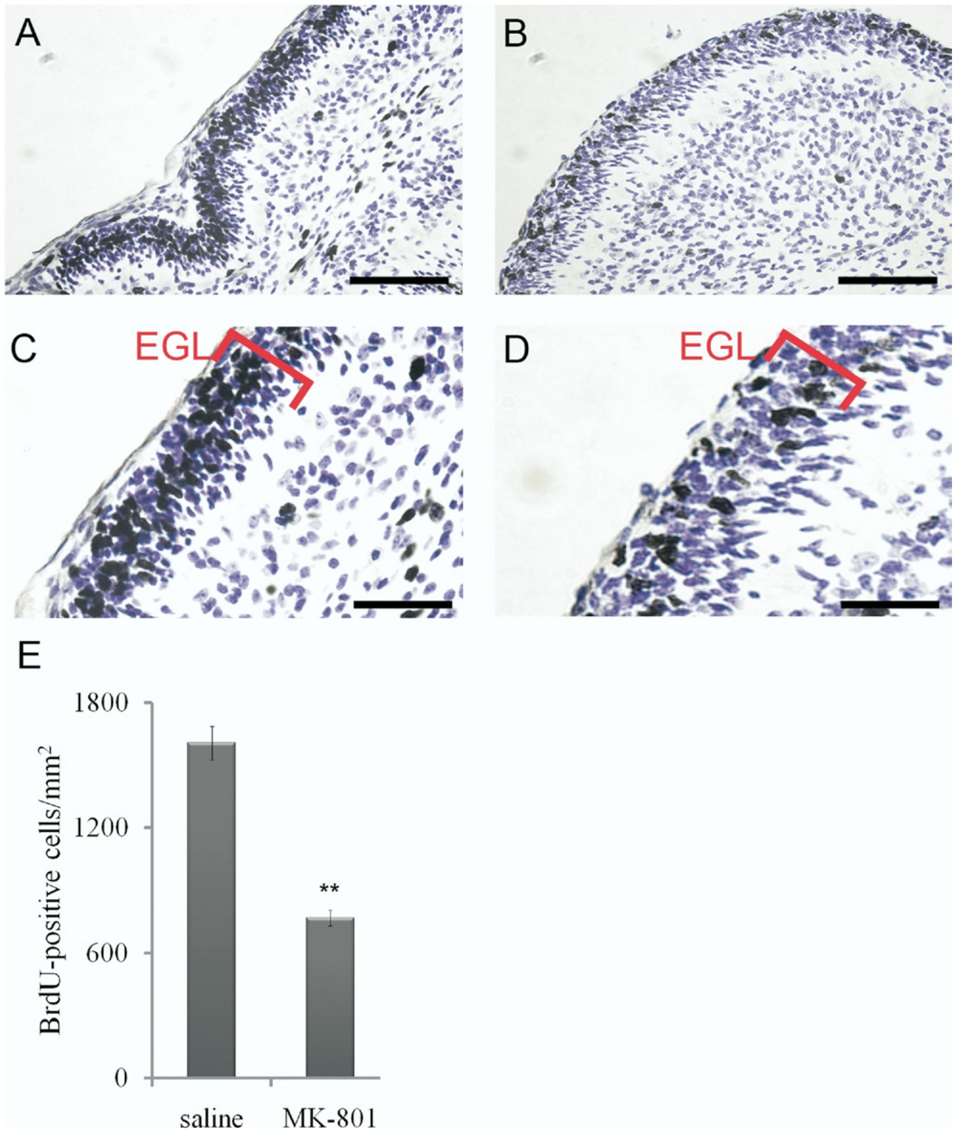

Fig. 4. BrdU labeling of EGL neurons. The pattern of BrdU labeling within the medial third of the cerebellum was examined at P8. (A, B) Typical pattern of BrdU staining observed 1 h following injection of the label (t=23 h) in mice treated with MK-801 or saline, respectively. BrdU-labeled cerebellar cross-sections were counterstained with thionin to delineate the proportion of BrdU-positive cells versus BrdU-negative cells within the EGL of saline- and MK-801-treated animals, respectively. Scale bars=200 μm. (C, D) Higher magnification view of the pattern of BrdU staining following (C) saline or (D) MK-801 treatment. Scale bars=100 μm. For each group, sagittal cross-sections through the EGL (red bracketed area) are shown between cerebellar lobes VI and VII. (E) Summary of BrdU-positive counts within the EGL of saline- and MK-801-treated mice (BrdU labeling performed 1 h prior to sacrifice). For (E) counts represent the average of numbers obtained from an analysis of two areas of 1 mm^2 from each section taken every 150 μm throughout the central third of the cerebellum for the animals in each group (N=4 animals/group). Asterisk in (E) indicates statistical significance between MK-801-treated mice and saline-treated counterparts (Student's t-test, ** $P<0.01$); error bars are shown ±S.E.M.

morphologic analyses: cerebellar volume, synapsin, calbindin, parvalbumin staining; data not shown).

MK-801-induced PCD within the EGL is dependent upon caspase-3

To better understand the mechanism by which MK-801-induced PCD occurred within the cerebellum, we examined the effect of MK-801 treatment in *Casp3*$^{-}$/$^{-}$ and wild-type littermates. *Casp3*$^{-}$/$^{-}$ mice (which show a reduction in developmental PCD within the embryonic forebrain) (Woo et al., 1998), exhibited morphologically normal cerebellar development, similar to wild-type controls (Fig. 6A and 6B, respectively). As performed above, counts of TUNEL positive cells were obtained from serial sections of the medial vermis lobes (lobes VI and VII) through the central third of the cerebellum (N≥9 animals/group). While ablation of caspase-3 did not significantly alter PCD within the IGL following MK-801 treatment at P8, loss of caspase-3 activity (in *Casp3*$^{-}$/$^{-}$ mice) dramatically reduced the levels of TUNEL positive cells within the EGL compared with wild-type controls (Fig. 6C and 6D). These data are summarized in Fig. 6E, and demonstrate that caspase-3 activity is both necessary and sufficient for the

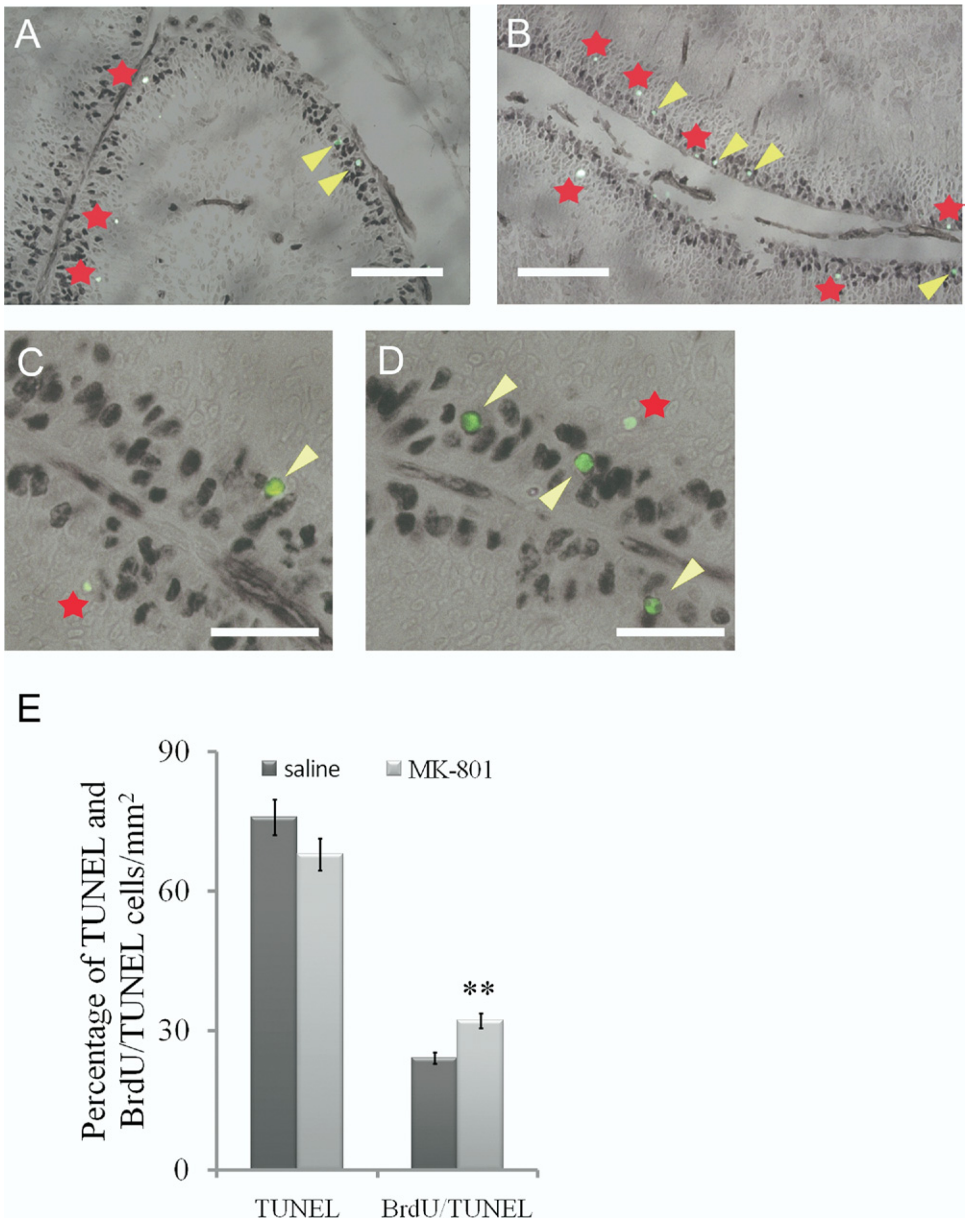

Fig. 5. Double labeling of EGL neurons with BrdU and TUNEL. The pattern of BrdU and TUNEL co-labeling within the medial third of the cerebellum was examined at P8. (A, B) Photomicrographs of concurrent TUNEL/BrdU in cerebellar cross-sections in (A) saline-, and (B) MK-801-treated animals. High magnification view of concurrent TUNEL/BrdU in representative cross-sections in (A) saline-, and (B) MK-801-treated animals. For (A–D) double-positive BrdU/TUNEL cells within the EGL in are indicated by arrowheads. TUNEL-positive/BrdU-negative cells are denoted by stars. Scale bars=200 μm (A, B); 50 μm (C, D). (E) Percent distribution of TUNEL-positive/BrdU-negative versus BrdU/TUNEL double positive cells in saline- and MK-801-treated animals. For (C) counts represent an average of the numbers obtained from analysis of two sections of 1 mm^2 on each 150 μm interval throughout the central third of the cerebellum for animals in each group (N=4 animals/group). Double asterisk in (E) indicates statistical significance between MK-801-treated mice and saline-treated counterparts (Student's t-test, ** P<0.01); error bars are shown ±S.E.M.

occurrence of MK-801-induced PCD within the EGL. Interestingly, within the EGL loss of caspase-3 reduced the numbers of TUNEL-positive cells (in both the saline and MK-801 treatment conditions) to levels below that seen in saline-treated *Casp3*$^{+/+}$ mice (Fig. 7E). Thus, in addition to preventing MK-801-mediated cell death, these data demonstrate that at least a subpopulation (~40%) of cells within the neonatal EGL requires caspase-3 to undergo developmental PCD. In contrast, within the more mature granule neurons of the IGL, loss of caspase-3 did not alter the pattern of developmental PCD; suggesting that they are capable of undergoing a caspase-3-independent form of PCD.

Inhibition of muscarinic receptors prevents MK-801 induced PCD within the EGL

The above results demonstrate that within a specific developmental window, MK-801 induced a marked increase in

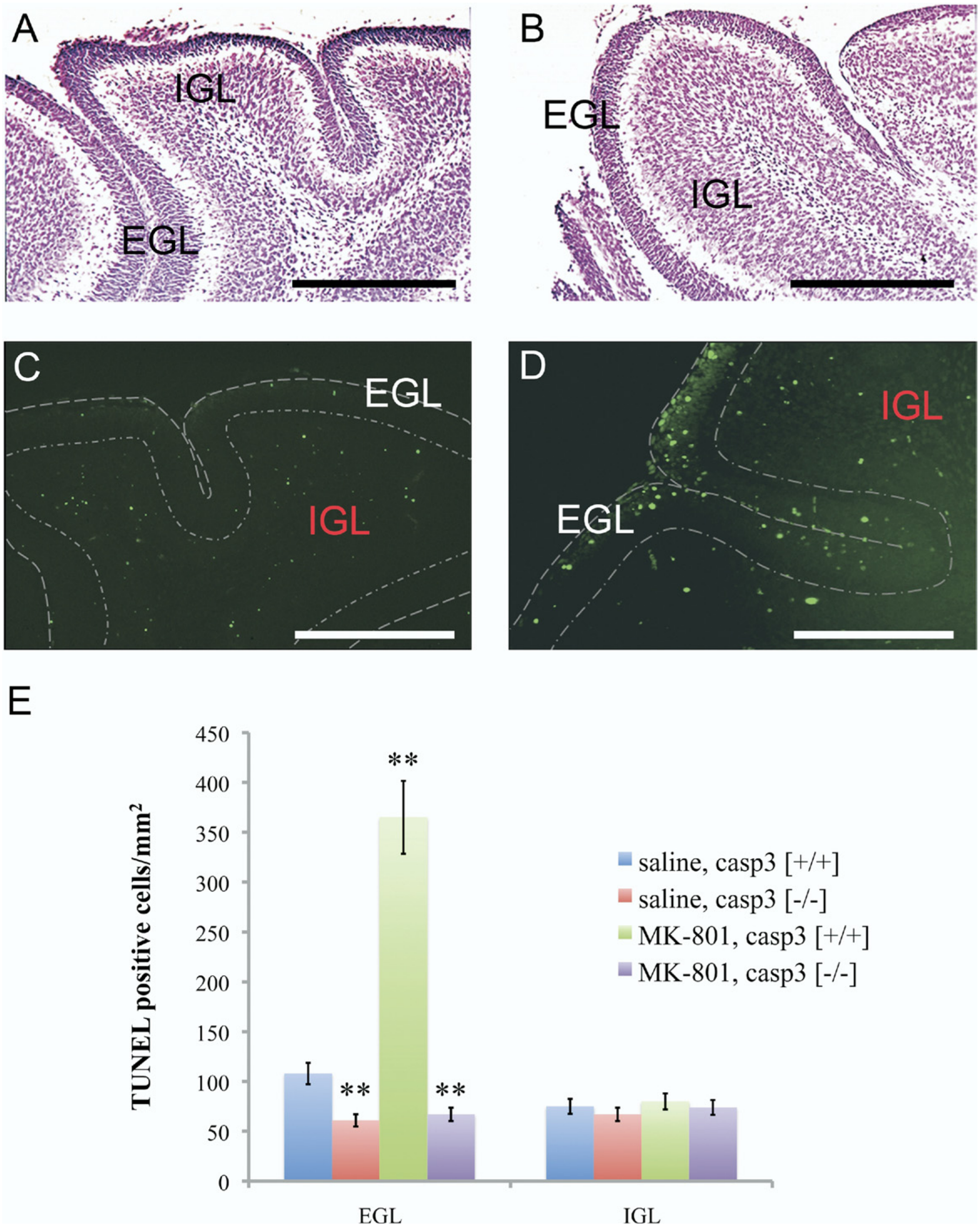

Fig. 6. MK-801-induced PCD within the EGL at P8 is dependent upon caspase-3. The pattern of MK-801-induced PCD was examined in *Casp3*$^{-}$/$^{-}$ mice and controls. (A, B) Photomicrographs of *Casp3*$^{-}$/$^{-}$ (A), and wild-type cerebella (B), at P8 exhibit similar morphology with respect to cerebellar structure. (C, D) Photomicrographs of TUNEL-positive cells within the cerebellum of *Casp3*$^{-}$/$^{-}$ (C), and wild-type littermates (D) following MK-801 treatment. Long dashed line delineates cerebellar outer boundary, short dashed line identifies Purkinje layer of the cerebellum. (E) Plot of the average number of TUNEL positive neurons per mm^2 (per animal) in each group within the EGL and IGL and IGLs of the cerebellum in *Casp3*$^{+/+}$ mice treated with saline (N=9), *Casp3*$^{+/+}$-treated mice treated with MK-801 (N=12), and *Casp3*$^{-}$/$^{-}$ mice treated with MK-801 (N=9). Error bars are shown ±S.E.M. Asterisks denote significant difference (one-way ANOVA, ** P<0.01) between treatment group and cognate saline controls. For photomicrographs (A–D), scale bar=400 μm.

PCD within the EGL, which occurred via a requisite caspase-3-dependent pathway. However these findings do not address the upstream mechanisms which induce caspase-3-dependent PCD following NMDA-receptor inhibition. In order to understand this mechanism, P7 animals were treated with the muscarinic antagonist scopolamine, or the GABAergic

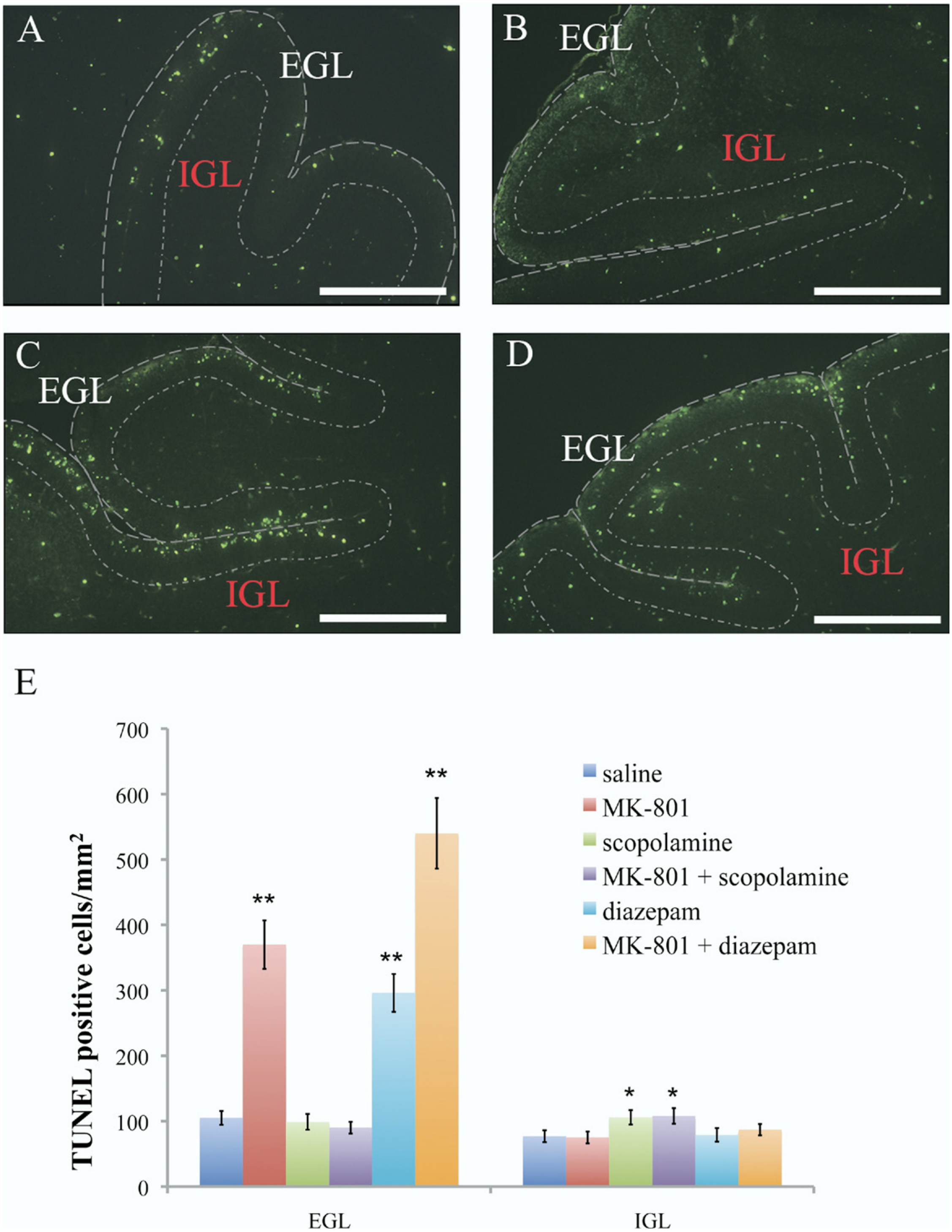

Fig. 7. Effects of scopolamine and diazepam-treatment on MK-801-induced PCD. Photomicrographs show TUNEL-labeling in cerebellar cross-sections from mice treated with (A) MK-801, (B) MK-801 plus scopolamine, (C) diazepam plus MK-801, (D) diazepam alone. Long dashed line delineates cerebellar outer boundary, short dashed line indicates Purkinje layer of the cerebellum. (E) Plot of the average number of TUNEL-positive cells per mm^2 for animals in each group within the EGL and IGL for the indicated drug combination. N=9 for saline, N=12 for MK-801, N=8 for scopolamine+MK-801, diazepam+MK-801, and diazepam treatment groups. For each group, N refers to the number of animals examined, each of which comprises data accumulated from a minimum of 14 sections (seven on either side of the midline) at intervals of 150 μm taken through the central third of the cerebellum at P8. Error bars are shown ±S.E.M. For photomicrographs (A–E), scale bar=200 μm. Statistical differences between groups were analyzed though one-way ANOVA; using pairwise multiple comparison procedures: Tukey test; * P<0.05, ** P<0.01.

agonist diazepam in the presence or absence of MK-801 (N=8 animals/group). As shown in Fig. 7, MK-801-induced cell death (Fig. 7A) was suppressed by *in vivo* scopolamine treatment (Fig. 7B), whereas treatment with diazepam significantly enhanced levels of MK-801-mediated cell death within the EGL (Fig. 7C). Indeed, diazepam treatment alone was found to significantly enhance PCD within the EGL of the P8 cerebellum (Fig. 7D). The level of PCD observed in mice treated with diazepam alone (Fig. 7E) was observed to be approximately 80% of that seen with MK-801. Stereotactic counts obtained from the central third of the cerebellum following scopolamine and diazepam treatments are summarized in Fig. 7E. These data demonstrate that MK-801-induced cell death was exacerbated by treatment with GABAergic agonists, and suppressed by scopolamine treatment. Similar to the results seen in *Casp3*$^{-}$/$^{-}$ mice, treatment with diazepam alone or concurrently with MK-801 did not significantly alter levels of PCD within the IGL. However, a trend toward greater numbers of TUNEL-positive cells within the IGL was observed following scopolamine treatment, which was statistically significant at the level of $P \leq 0.05$.

DISCUSSION

In the present study, we have analyzed the effects of exposing the neonatal murine CNS to the non-competitive NMDA antagonist MK-801 for a period of 24 h. Neonatal application of MK-801 has previously been shown to induce cell death in rat (Ikonomidou et al., 1999). In mice, maximal induction of MK-801-induced cell death was observed from P7-8, application outside this window (P3, P10) did not result in a significant elevation of cell death in the CNS. We extended our analysis of MK-801-induced effects to the metencephalon, a region not previously examined in rodents. Treatment with MK-801 led to substantial cell death within EGL of the cerebellum. Dying cells in this region exhibited both morphologic and functional (TUNEL staining, caspase-3 activity) hallmarks of PCD.

The EGL constitutes a secondary germinal zone during early postnatal development. By P8, cerebellar stem cells have given rise to a layer consisting primarily of granule cell progenitors, producing immature or pre-migratory granule cells, which develop into migratory granule neurons (Carletti and Rossi, 2008). Gradually, the EGL becomes depleted by 3–4 weeks postnatally, ultimately giving way to the mature molecular layer of the cerebellum. Analysis of the P8 cerebellum demonstrates that a substantial population of TUNEL positive cells could be identified through BrdU labeling for $\geq$1 h prior to examination (31%, largely representing granule cell progenitors based upon their localization to the pial surface of the EGL). Analysis of TUNEL and BrdU/TUNEL positive cells in MK-801- and saline-treated animals in the EGL indicates that MK-801 treatment does not substantially alter the population of cells undergoing PCD; but instead increases the probability of cell death. The lack of increased cell death within the IGL upon MK-801 treatment suggests that it is the granule cell progenitors and pre-migratory granule cells, which are sensitive to NMDA-receptor blockade, and that the post-migratory granule cells are far more resistant to these effects. These findings are corroborated by a recent study, which demonstrates that the sensitivity of isolated immature granule neurons to MK-801 decreased as a function of the number of days these neurons were maintained *in vitro* (Klimaviciusa et al., 2008*).* Thus as the granule cells mature, they undergo a fundamental change in their response to NMDA receptor-mediated signaling. Several factors may account for this change in sensitivity. First, the influence of NMDA-mediated glutamate signaling is significantly larger in immature granule cells of the EGL than mature granule neurons of the IGL; owing to greater AMPA channel activity in mature neurons (D'Angelo et al., 1993). Thus, alterations in NMDA-mediated depolarization have a proportionally larger influence on membrane potential in immature neurons of the EGL, than mature granule neurons of the IGL. Second, mature granule neurons receive an array of synaptic inputs; in contrast to immature granule cells. This effect may stabilize the influence of any particular form of synaptic (such as NMDA-mediated) input with respect to changes in the membrane potential. Finally, changes in the subunit composition of NMDA receptors from NR2B to NR2A and NR2C (Farrant et al., 1994; Cathala et al., 2000), which occur during the migratory transition between immature and mature granule cells, may alter the sensitivity of these cells to undergo PCD in response to changes in excitatory tonus.

A wide array of cellular signals have been shown to be capable of inducing PCD (Adams, 2003). A major point of convergence for these pathways lies at the level of executioner caspases (caspase-3, -6 and -7) (Slee et al., 2001; Lakhani et al., 2006). Many forms of injury-induced neurodegeneration show redundant expression of executioner caspases (Zheng et al., 2000; Houde et al., 2004). Therefore, it is perhaps not surprising that for all forms of injury-induced neurodegeneration thus far examined, caspase-3 ablation (at best) may slow the temporal rate of PCD following injury; yet has minimal effects on altering the final levels of surviving neurons (D'Mello et al., 2000; Keramaris et al., 2000; Pompeiano et al., 2000; Selznick et al., 2000; Vanderluit et al., 2000; D'Sa-Eipper et al., 2001; Zaidi et al., 2001a,b; Le et al., 2002; D'Sa et al., 2003; Nowoslawski et al., 2005; Young et al., 2005; West et al., 2006). By contrast, MK-801-induced PCD within the EGL is the first neurodegenerative example which exhibits an absolute requirement for caspase-3 activity.

Within the IGL, loss of caspase-3 activity showed no effect on the extent of developmental PCD observed. This is not due to an absence of caspase-3 expression, as caspase-3 is observed within IGL neurons at this stage. In contrast, a subpopulation of cells within the EGL requires caspase-3 activation to undergo developmental PCD, indicating that PCD signaling responses become modified in cerebellar granule cells during maturation; similar to the results obtained with MK-801. Despite their different inductive mechanisms, it appears that it is the more embryonic granule populations which are sensitive to the effects of MK-801 exposure and caspase-3 ablation.

The principal model of cell death following NMDA inhibition involves excitatory disinhibition (Morimoto et al., 2004). In this model, blockade of NMDA receptors by MK-801 in a given neuron, results in reduced activation of downstream (post-synaptic) targets. If these post-synaptic neurons are inhibitory in nature, then the net effect will be a reduction in inhibitory input to tertiary neuronal targets. If this reduction is of sufficient magnitude and duration, excitotoxicity can result (Chittajallu et al., 2007). These targets typically represent non-NMDA excitatory neurons such as cholinergic neurons. While this model sufficiently explains the injurious effects of MK-801 in the adult CNS (Giovannini et al., 1994), this is unlikely to be the operant mechanism of MK-801-induced cell injury within the EGL. The targets of MK-801 treatment within the EGL (granule cell progenitors and pre-migratory granule cells) do not exhibit meaningful integration into the cerebellar synaptic network (Carletti and Rossi, 2008). Consistent with this, the more mature granule population within the IGL exhibits reduced, not enhanced, sensitivity to MK-801. Instead we propose that the effects of MK-801 reflect the requirement of EGL neurons for threshold levels of neuronal responsiveness.

While EGL neurons are incapable of producing an action potential, these cells do exhibit an oscillatory Ca^{2+} current known to be required for cell migration, and whose amplitude can be depressed by both transient (4 h) inhibition of Ca^{2+} influx via NMDA receptors or by preventing Ca^{2+} release from intracellular stores (Komuro and Rakic, 1993, 1996). We hypothesized that a combination of voltage and ligand-gated ion channels may act to cooperatively regulate the survival of EGL neurons via their effects on intracellular Ca^{2+} levels. To examine the role of the intrinsic oscillatory Ca^{2+} current of EGL neurons in regulating PCD, we investigated the effects of the muscarinic antagonist scopolamine, and the GABAergic agonist diazepam, in the presence and absence of MK-801 *in vivo*. Scopolamine treatment inhibited MK-801-induced PCD within the EGL. Within developing granule neurons, scopolamine antagonizes the actions of muscarinic (G-protein coupled) receptors primarily represented by the M2 and M3 class receptors within EGL neurons during this period (Alonso et al., 1990; McLeskey and Wojcik, 1992; Court et al., 1995; Yan et al., 1995). The principal ion channels regulated by these receptors are G-protein sensitive inwardly rectifying potassium channels (GIRKs), which play an important role in regulating neuronal responsiveness through the regulation of potassium efflux (Ehrengruber et al., 1997). The application of scopolamine, therefore, tends to counteract the effects of MK-801 and preserve the Ca^{2+} current by blocking an important source of cellular hyperpolarization. This leads to a subsequent increase in intracellular Ca^{2+} via voltage-gated Ca^{2+} channels (Guatteo et al., 2004), thus counterbalancing the inhibitory effects of MK-801 on Ca^{2+} influx via NMDA channels. By contrast diazepam, which mimics the actions of GABA, enhances the duration of chloride channel opening in GABA receptors expressed on migrating granule neurons (Zdilar et al., 1992); this in turn acts to hyperpolarize the cell and prevent the rise of intracellular Ca^{2+} mediated via voltage-gated Ca^{2+} channels. Consistent with this, we observed that diazepam treatment alone or in combination with MK-801 treatment, dramatically enhanced PCD within the EGL. These data suggest that sustained depression of neuronal responsiveness below a given set point within EGL neurons may induce the caspase-3-dependent PCD observed.

Unlike the EGL, MK-801 treatment alone, or in combination with diazepam did not affect levels of PCD within granule neurons of the IGL. In contrast, ethanol administration during the early postnatal period in rats has been reported to result in a robust enhancement of PCD within both EGL and IGL neurons of the cerebellum (Nowoslawski et al., 2005). The differential effects of MK-801 versus ethanol in the cerebellum are interesting given the ability of ethanol to simultaneously inhibit NMDA receptors (Peoples and Weight, 1995), activate $GABA_A$ channels (Wick et al., 1998; Mihic, 1999), and directly stimulate GIRKs through C-terminal binding which bypasses their normal regulation by metabotropic receptors (Kobayashi et al., 1999; Lewohl et al., 1999; Blednov et al., 2001). These combined actions of ethanol, each acting to depress neuronal excitability, may *in toto* sufficiently overwhelm the more robust set point system within mature granule neurons to initiate PCD. Taken together, the results suggest that the neurodegenerative effects of neonatal ethanol administration in granule neurons may be due to its influence on inwardly rectifying potassium currents as much as it effects on NMDA or GABA currents. While the results demonstrate that caspase-3 is both necessary and sufficient to regulate NMDA-activity-dependent PCD in granule cell progenitors *in vivo*; it will be interesting to see what role this mechanism plays in controlling ethanol-induced neurodegeneration.

REFERENCES

Abraham H, Tornoczky T, Kosztolanyi G, Seress L (2001) Cell formation in the cortical layers of the developing human cerebellum. Int J Dev Neurosci 19:53–62.

Adams JM (2003) Ways of dying: multiple pathways to apoptosis. Genes Dev 17:2481–2495.

Alonso R, Didier M, Soubrie P (1990) [3H]N-methylscopolamine binding studies reveal M2 and M3 muscarinic receptor subtypes on cerebellar granule cells in primary culture. J Neurochem 55: 334–337.

Baehrecke EH (2002) How death shapes life during development. Nat Rev Mol Cell Biol 3:779–787.

Bayer SA, Altman J, Russo RJ, Zhang X (1993) Timetables of neurogenesis in the human brain based on experimentally determined patterns in the rat. Neurotoxicology 14:83–144.

Blednov YA, Stoffel M, Chang SR, Harris RA (2001) Potassium channels as targets for ethanol: studies of G-protein-coupled inwardly rectifying potassium channel 2 (GIRK2) null mutant mice. J Pharmacol Exp Ther 298:521–530.

Carletti B, Rossi F (2008) Neurogenesis in the cerebellum. Neuroscientist 14:91–100.

Cathala L, Misra C, Cull-Candy S (2000) Developmental profile of the changing properties of NMDA receptors at cerebellar mossy fiber-granule cell synapses. J Neurosci 20:5899–5905.

Chittajallu R, Kunze A, Mangin JM, Gallo V (2007) Differential synaptic integration of interneurons in the outer and inner molecular layers of the developing dentate gyrus. J Neurosci 27:8219–8225.

Court JA, Perry EK, Spurden D, Griffiths M, Kerwin JM, Morris CM, Johnson M, Oakley AE, Birdsall NJ, Clementi F, et al. (1995) The role of the cholinergic system in the development of the human cerebellum. Brain Res Dev Brain Res 90:159–167.

D'Angelo E, Rossi P, Taglietti V (1993) Different proportions of N-methyl-D-aspartate and non-N-methyl-D-aspartate receptor currents at the mossy fibre-granule cell synapse of developing rat cerebellum. Neuroscience 53:121–130.

D'Mello SR, Kuan CY, Flavell RA, Rakic P (2000) Caspase-3 is required for apoptosis-associated DNA fragmentation but not for cell death in neurons deprived of potassium. J Neurosci Res 59: 24–31.

D'Sa C, Klocke BJ, Cecconi F, Lindsten T, Thompson CB, Korsmeyer SJ, Flavell RA, Roth KA (2003) Caspase regulation of genotoxin-induced neural precursor cell death. J Neurosci Res 74:435–445.

D'Sa-Eipper C, Leonard JR, Putcha G, Zheng TS, Flavell RA, Rakic P, Kuida K, Roth KA (2001) DNA damage-induced neural precursor cell apoptosis requires p53 and caspase 9 but neither Bax nor caspase 3. Development 128:137–146.

Dobbing J, Sands J (1979) Comparative aspects of the brain growth spurt. Early Hum Dev 3:79–83.

Ehrengruber MU, Doupnik CA, Xu Y, Garvey J, Jasek MC, Lester HA, Davidson N (1997) Activation of heteromeric G protein-gated inward rectifier K^+ channels overexpressed by adenovirus gene transfer inhibits the excitability of hippocampal neurons. Proc Natl Acad Sci U S A 94:7070–7075.

Farrant M, Feldmeyer D, Takahashi T, Cull-Candy SG (1994) NMDA-receptor channel diversity in the developing cerebellum. Nature 368:335–339.

Giovannini MG, Mutolo D, Bianchi L, Michelassi A, Pepeu G (1994) NMDA receptor antagonists decrease GABA outflow from the septum and increase acetylcholine outflow from the hippocampus: a microdialysis study. J Neurosci 14:1358–1365.

Goldowitz D, Hamre K (1998) The cells and molecules that make a cerebellum. Trends Neurosci 21:375–382.

Gottlieb A, Keydar I, Epstein HT (1977) Rodent brain growth stages: an analytical review. Biol Neonate 32:166–176.

Greensmith L, Mentis GZ, Vrbova G (1994) Blockade of N-methyl-D-aspartate receptors by MK-801 (dizocilpine maleate) rescues motoneurones in developing rats. Brain Res Dev Brain Res 81: 162–170.

Guatteo E, Bengtson CP, Bernardi G, Mercuri NB (2004) Voltage-gated calcium channels mediate intracellular calcium increase in weaver dopaminergic neurons during stimulation of D2 and GABAB receptors. J Neurophysiol 92:3368–3374.

Hahn ME, Walters JK, Lavooy J, DeLuca J (1983) Brain growth in young mice: evidence on the theory of phrenoblysis. Dev Psychobiol 16:377–383.

Hara MR, Snyder SH (2007) Cell signaling and neuronal death. Annu Rev Pharmacol Toxicol 47:117–141.

Houde C, Banks KG, Coulombe N, Rasper D, Grimm E, Roy S, Simpson EM, Nicholson DW (2004) Caspase-7 expanded function and intrinsic expression level underlies strain-specific brain phenotype of caspase-3-null mice. J Neurosci 24:9977–9984.

Ikonomidou C, Bosch F, Miksa M, Bittigau P, Vockler J, Dikranian K, Tenkova TI, Stefovska V, Turski L, Olney JW (1999) Blockade of NMDA receptors and apoptotic neurodegeneration in the developing brain. Science 283:70–74.

Ikonomidou C, Bittigau P, Ishimaru MJ, Wozniak DF, Koch C, Genz K, Price MT, Stefovska V, Horster F, Tenkova T, Dikranian K, Olney JW (2000) Ethanol-induced apoptotic neurodegeneration and fetal alcohol syndrome. Science 287:1056–1060.

Jackson IJ, Abbott CM (1999) Mouse genetics and transgenics: a practical approach. Oxford: Oxford University Press.

Keramaris E, Stefanis L, MacLaurin J, Harada N, Takaku K, Ishikawa T, Taketo MM, Robertson GS, Nicholson DW, Slack RS, Park DS (2000) Involvement of caspase 3 in apoptotic death of cortical neurons evoked by DNA damage. Mol Cell Neurosci 15:368–379.

Klimaviciusa L, Safiulina D, Kaasik A, Klusa V, Zharkovsky A (2008) The effects of glutamate receptor antagonists on cerebellar granule cell survival and development. Neurotoxicology 29:101–108.

Kobayashi T, Ikeda K, Kojima H, Niki H, Yano R, Yoshioka T, Kumanishi T (1999) Ethanol opens G-protein-activated inwardly rectifying K^+ channels. Nat Neurosci 2:1091–1097.

Komuro H, Rakic P (1993) Modulation of neuronal migration by NMDA receptors. Science 260:95–97.

Komuro H, Rakic P (1996) Intracellular Ca^{2+} fluctuations modulate the rate of neuronal migration. Neuron 17:275–285.

Lakhani SA, Masud A, Kuida K, Porter GA Jr, Booth CJ, Mehal WZ, Inayat I, Flavell RA (2006) Caspases 3 and 7: key mediators of mitochondrial events of apoptosis. Science 311:847–851.

Le DA, Wu Y, Huang Z, Matsushita K, Plesnila N, Augustinack JC, Hyman BT, Yuan J, Kuida K, Flavell RA, Moskowitz MA (2002) Caspase activation and neuroprotection in caspase-3-deficient mice after in vivo cerebral ischemia and in vitro oxygen glucose deprivation. Proc Natl Acad Sci U S A 99:15188–15193.

Lewohl JM, Wilson WR, Mayfield RD, Brozowski SJ, Morrisett RA, Harris RA (1999) G-protein-coupled inwardly rectifying potassium channels are targets of alcohol action. Nat Neurosci 2:1084–1090.

Mattson MP (2000) Apoptosis in neurodegenerative disorders. Nat Rev Mol Cell Biol 1:120–129.

Mattson MP (2003) Excitotoxic and excitoprotective mechanisms: abundant targets for the prevention and treatment of neurodegenerative disorders. Neuromol Med 3:65–94.

McIntosh TK, Vink R, Soares H, Hayes R, Simon R (1989) Effects of the N-methyl-D-aspartate receptor blocker MK-801 on neurologic function after experimental brain injury. J Neurotrauma 6:247–259.

McLeskey SW, Wojcik WJ (1992) Propylbenzilylcholine mustard has greater specificity for muscarinic m2 receptors than for m3 receptors present in cerebellar granule cell culture from rat. J Pharmacol Exp Ther 263:703–707.

Middleton FA, Strick PL (1998) The cerebellum: an overview. Trends Neurosci 21:367–369.

Mihic SJ (1999) Acute effects of ethanol on GABAA and glycine receptor function. Neurochem Int 35:115–123.

Morimoto K, Fahnestock M, Racine RJ (2004) Kindling and status epilepticus models of epilepsy: rewiring the brain. Prog Neurobiol 73:1–60.

Nicholls DG (2004) Mitochondrial dysfunction and glutamate excitotoxicity studied in primary neuronal cultures. Curr Mol Med 4: 149–177.

Nicholls DG, Ward MW (2000) Mitochondrial membrane potential and neuronal glutamate excitotoxicity: mortality and millivolts. Trends Neurosci 23:166–174.

Nowoslawski L, Klocke BJ, Roth KA (2005) Molecular regulation of acute ethanol-induced neuron apoptosis. J Neuropathol Exp Neurol 64:490–497.

Peoples RW, Weight FF (1995) Cutoff in potency implicates alcohol inhibition of N-methyl-D-aspartate receptors in alcohol intoxication. Proc Natl Acad Sci U S A 92:2825–2829.

Pompeiano M, Blaschke AJ, Flavell RA, Srinivasan A, Chun J (2000) Decreased apoptosis in proliferative and postmitotic regions of the caspase 3-deficient embryonic central nervous system. J Comp Neurol 423:1–12.

Selznick LA, Zheng TS, Flavell RA, Rakic P, Roth KA (2000) Amyloid beta-induced neuronal death is bax-dependent but caspase-independent. J Neuropathol Exp Neurol 59:271–279.

Slee EA, Adrain C, Martin SJ (2001) Executioner caspase-3, -6, and -7 perform distinct, non-redundant roles during the demolition phase of apoptosis. J Biol Chem 276:7320–7326.

Tanaka M, Marunouchi T (1998) Immunohistochemical analysis of developmental stage of external granular layer neurons which undergo apoptosis in postnatal rat cerebellum. Neurosci Lett 242:85–88.

Vanderluit JL, McPhail LT, Fernandes KJ, McBride CB, Huguenot C, Roy S, Robertson GS, Nicholson DW, Tetzlaff W (2000) Caspase-3 is activated following axotomy of neonatal facial motoneurons and caspase-3 gene deletion delays axotomy-induced cell death in rodents. Eur J Neurosci 12:3469–3480.

West T, Atzeva M, Holtzman DM (2006) Caspase-3 deficiency during development increases vulnerability to hypoxic-ischemic injury through caspase-3-independent pathways. Neurobiol Dis 22: 523–537.

Wick MJ, Mihic SJ, Ueno S, Mascia MP, Trudell JR, Brozowski SJ, Ye Q, Harrison NL, Harris RA (1998) Mutations of gamma-aminobutyric acid and glycine receptors change alcohol cutoff: evidence for an alcohol receptor? Proc Natl Acad Sci U S A 95:6504–6509.

Woo M, Hakem R, Soengas MS, Duncan GS, Shahinian A, Kagi D, Hakem A, McCurrach M, Khoo W, Kaufman SA, Senaldi G, Howard T, Lowe SW, Mak TW (1998) Essential contribution of caspase 3/CPP32 to apoptosis and its associated nuclear changes. Genes Dev 12:806–819.

Yan GM, Lin SZ, Irwin RP, Paul SM (1995) Activation of muscarinic cholinergic receptors blocks apoptosis of cultured cerebellar granule neurons. Mol Pharmacol 47:248–257.

Young C, Roth KA, Klocke BJ, West T, Holtzman DM, Labruyere J, Qin YQ, Dikranian K, Olney JW (2005) Role of caspase-3 in ethanol-induced developmental neurodegeneration. Neurobiol Dis 20: 608–614.

Yuan J (2006) Divergence from a dedicated cellular suicide mechanism: exploring the evolution of cell death. Mol Cell 23:1–12.

Zaidi AU, McDonough JS, Klocke BJ, Latham CB, Korsmeyer SJ, Flavell RA, Schmidt RE, Roth KA (2001a) Chloroquine-induced neuronal cell death is p53 and Bcl-2 family-dependent but caspase-independent. J Neuropathol Exp Neurol 60:937–945.

Zaidi AU, D'Sa-Eipper C, Brenner J, Kuida K, Zheng TS, Flavell RA, Rakic P, Roth KA (2001b) Bcl-X(L)-caspase-9 interactions in the developing nervous system: evidence for multiple death pathways. J Neurosci 21:169–175.

Zdilar D, Luntz-Leybman V, Frostholm A, Rotter A (1992) Differential expression of GABAA/benzodiazepine receptor beta 1, beta 2, and beta 3 subunit mRNAs in the developing mouse cerebellum. J Comp Neurol 326:580–594.

Zheng TS, Hunot S, Kuida K, Momoi T, Srinivasan A, Nicholson DW, Lazebnik Y, Flavell RA (2000) Deficiency in caspase-9 or caspase-3 induces compensatory caspase activation. Nat Med 6:1241–1247.

APPENDIX

Supplementary data

Supplementary data associated with this article can be found, in the online version, at doi:10.1016/j.neuroscience.2008.10.062.

(Accepted 29 October 2008)
(Available online 8 November 2008)